electronic reprint

Acta Crystallographica Section D
Biological Crystallography
ISSN 0907-4449
Editors: **E. N. Baker and Z. Dauter**

The role of solvent transport in cryo-annealing of macromolecular crystals

Douglas H. Juers and Brian W. Matthews

Acta Crystallographica Section D
Biological Crystallography
ISSN 0907-4449

The role of solvent transport in cryo-annealing of macromolecular crystals

Douglas H. Juers and Brian W. Matthews*

Institute of Molecular Biology, Howard Hughes Medical Institute and Department of Physics, 1229 University of Oregon, Eugene, OR 97403-1229, USA

Correspondence e-mail: brian@uoxray.uoregon.edu

Received 15 September 2003
Accepted 8 December 2003

Macromolecular crystals are usually cooled to ~100 K for X-ray diffraction experiments in order to diminish lattice damage arising from the ionizing radiation. Such cooling often produces lattice disorder, but this disorder can sometimes be substantially reduced by cycling the crystal between low and higher temperatures (called annealing). Here, two related aspects of cryocooling and annealing are investigated using crystals of β-galactosidase and thermolysin. Firstly, as has been reported with other systems, there is an optimal cryoprotectant concentration above and below which diffraction is poor, with high mosaicity, diffuse scatter and low signal to noise. Measurements of the bulk density of the respective cryosolvents are consistent with the idea that at the optimal cryoprotectant concentration the contraction of the bulk solvent on cooling largely compensates for the contraction of the macromolecular lattice. Secondly, by controlling the relative humidity of the gas that contacts the crystal during the high (room) temperature phase, it is found that water is either imported into or exported out of the crystals during the melting phase of annealing. This water transport appears to change the concentration of the cryoprotectant solution and in so doing alters its thermal contraction. Thus, annealing appears to be involved, at least in part, in the tuning of the thermal contraction of the bulk solvent to best compensate for lattice contraction. Furthermore, it is found that if the cryoprotectant concentration is initially too high then annealing is more successful than if the concentration is initially too low. This result suggests that the search for optimal cryoprotectant conditions may be facilitated by equilibration of the crystal to relatively high cryoprotectant concentration followed by annealing.

1. Introduction

Flash-cooling of macromolecular crystals for X-ray diffraction experiments has become common practice in the past decade because the crystals are more resistant to X-ray damage at low temperature (Haas & Rossmann, 1970; Hope, 1988; Rodgers, 1994; Garman & Schneider, 1997; Garman, 1999). This process is particularly useful for situations requiring longer X-ray exposures, such as the use of small crystals or MAD data collection. Although several different variations of flash-cooling have been described, the technique is not always straightforward and is often itself damaging to the crystal lattice. The causes of such damage are incompletely understood, with possible explanations including ice formation, strain arising from uneven cooling and differential expansion of the bulk solvent and crystal lattice (Juers & Matthews, 2001; Kriminski *et al.*, 2002).

In some cases, lattice damage from the initial cooling can be reduced by cycling the crystal between the initial low-temperature state and some higher temperature. Termed annealing, several variants of this technique have been described (Harp *et al.*, 1998, 1999; Yeh & Hol, 1998; Kriminski *et al.*, 2002). In some cases the results are quite dramatic, allowing the collection of high-resolution diffraction data which otherwise may have been impossible.

Although annealing is clearly useful in some cases, its mechanism is not well understood. Basing their hypothesis on X-ray topography in concert with line-shape measurements, Kriminski *et al.* (2002) suggested that annealing involves the growth of domain sizes at the higher temperature. They also proposed possible mechanisms to account for the growth. Here, we present experiments designed to investigate the role of humidity in one type of annealing. The results suggest that changes in bulk-solvent composition caused by water transport at the higher temperature are at least in part responsible for changes in diffraction quality.

2. Materials and methods

2.1. Crystals of *Escherichia coli* β-galactosidase and thermolysin

Unless otherwise noted, all chemicals were purchased from Sigma. Crystals of the orthorhombic form of *E. coli* β-galactosidase were grown as described previously (Juers *et al.*, 2000) using vapor diffusion in hanging drops with polyethylene glycol (PEG) 8000 (Hampton Research, Laguna Niguel, CA, USA) as the precipitant. After growth for 1–2 weeks at 288 K, the crystals were harvested into a storage buffer consisting of 100 m*M* bis-Tris pH 6.5, 200 m*M* $MgCl_2$, 100 m*M* NaCl, 10 m*M* DTT (BioVectra DCL, Oxford, CT, USA) and 10%(*w*/*v*) PEG 8000 and stored at room temperature. Flash-cooling in the crystal-growth buffer was tried both with and without viscous oils (Parabar 10312, also called Paratone N from Exxon Chemical, Houston, TX, USA; now sold as Infineum v8512 by Infineum, Linden, NJ, USA; Fomblin YR-1800, Lancaster Synthesis, Windham, NH, USA) (Hope, 1988) in order to remove the buffer surrounding the crystal. In all cases, the lattice order was greatly compromised, with diffraction spots persisting to only 10 Å resolution, in comparison with room-temperature diffraction beyond 3.0 Å both with and without the oils. This outcome necessitated the search for cryoprotectants.

Several different compounds (glycerol, PEG 400, ethylene glycol, PEG 550 monomethyl ether, 2-methyl-2-4-pentanediol, glucose, sucrose and dimethyl sulfoxide) were tried by briefly (1–4 s) passing the crystal through the cryoprotectant. Using this technique, the most promising cryoprotectant was dimethyl sulfoxide (DMSO). Subsequently, we found that by slowly equilibrating the crystal to approximately 30%(*v*/*v*) DMSO, flash-cooling could be carried out well enough to collect data to beyond 1.5 Å resolution. Subsequent studies showed that 40%(*v*/*v*) PEG 400 can also serve as a good cryoprotectant.

Crystals of the hexagonal form of thermolysin were grown as described previously (Hausrath & Matthews, 2002) using vapor diffusion in sitting drops with water as the precipitant. After growth at room temperature for a few days, the cystals were harvested into a storage buffer of 25 m*M* MES [2-(*N*-morpholino)ethanesulfonic acid] pH 6.0, 500 m*M* NaCl, 1 m*M* $CaCl_2$ and stored at room temperature. On a home source, these crystals diffract to a resolution of 1.6–1.8 Å at room temperature. The crystals can be flash-cooled without cryoprotectants using Fomblin YR-1800 to remove the surrounding solvent. However, the lattice order is compromised, with increased mosaicity and a diffraction limit of ∼2.5 Å.

After some searching, it was found that glucose can act as a good cryoprotectant for thermolysin, working best at 60%(*w*/*v*) in concert with Fomblin YR1800 to remove the mother liquor on the outside of the crystal. With this combination, the thermolysin crystals can be successfully flash-cooled and data sets to 1.1 Å resolution can be collected. Crystals flash-cooled with glucose but without Fomblin do not diffract as well and have higher mosaicity, regardless of the glucose concentration.

For equilibration with cryoprotectants, the crystals were first placed in a vial of mother liquor (∼1 ml) with no cryoprotectant (either 70 or 100% of the storage buffer for β-galactosidase; 100% of the storage buffer for thermolysin). The cryoprotectant equilibration was then carried out in 2–5% increments. With the crystals sitting on one side of the vial, either pure cryoprotectant or mother liquor with cryoprotectant added was introduced on the other side of the vial and mixed. The mixture was allowed to equilibrate for 30–90 min and the process was repeated until the cryoprotectant concentration was ∼2–3% lower than the target. The crystals were then transferred to another vial, which contained a solution with the target cryoprotectant concentration. For β-galactosidase, the final solution conditions were 70 m*M* bis-Tris pH 6.5, 140 m*M* $MgCl_2$, 70 m*M* NaCl, 7 m*M* DTT, 7%(*w*/*v*) PEG 8000 and *x*%(*v*/*v*) cryoprotectant, where *x* ranged from 0 to 50. For thermolysin, the final solution conditions were 25 m*M* MES pH 6.0, 500 m*M* NaCl, 1 m*M* $CaCl_2$, *x*%(*w*/*v*) glucose, where *x* ranged from 0 to 60. Here, *x*%(*w*/*v*) means *x* grams of anhydrous glucose per 100 ml of solution.

2.2. Annealing with humidity control

In a cryo-annealing experiment, the crystal is initially cooled and then cycled between the low temperature and some higher temperature. Three variations of the annealing process have been described. In the first, the cryostream is blocked and the crystal warms in place before being recooled in the cryostream (Yeh & Hol, 1998). In the second, when the cryostream is blocked, the crystal is removed from the loop and allowed to incubate in a cryosolution at room temperature before being remounted in the cryostream (Harp *et al.*, 1998, 1999). More recently, a third variation has been described in

which the crystal is left in the loop but the high temperature is restricted to 230–250 K (Kriminski *et al.*, 2002).

In the experiments described here, the crystals were mounted by scooping into a small polyethylene loop (Teng, 1990; Hampton Research) and blotting in order to minimize the amount of surrounding solution. In each case, a loop somewhat smaller than the crystal was used, making it easier to minimize the amount of mother liquor surrounding the crystal. Crystal dimensions were typically 0.1–0.3 mm on each side for β-galactosidase and 0.1–0.2 mm in rod diameter for thermolysin. In the case of thermolysin with or without cryoprotectant, the crystal was sometimes first transferred to a pool of Fomblin YR-1800 and the surrounding mother liquor was drawn off with a thin glass tube. In all cases, initial cooling was carried out to $\sim$100 K by blocking (*i.e.* interrupting) the cryostream, placing the crystal on the goniometer and restoring the cryostream. Annealing was then performed using the first method described above, in which the crystal is left in the loop while the cryostream is blocked, cycling the crystal between $\sim$100 and $\sim$300 K. Two parameters in the annealing procedure were varied: the blocking time and the relative humidity of the room-temperature gas contacting the crystal during the blocking phase.

Two methods were used to control the relative humidity. In the first, a room-temperature nitrogen flow was directed at the crystal. The relative humidity of this gas flow was controlled by mixing dry and humid nitrogen in various proportions. Variations of this technique have been described previously (Kiefersauer *et al.*, 2000; Sjögren *et al.*, 2002). The humid flow was turned off while the crystal was at low temperature and turned on while the cryostream was blocked. Although this method gave interesting results, some of which are described below, there were ambiguities involved in synchronizing the blocking of the cryostream with the activation of the humid flow. The second method, which eliminates these ambiguities, was to use a humidity chamber. A box was constructed from Mylar and duct tape, with ports for the X-ray beam, the incoming cryostream, the outgoing cryostream, a humid nitrogen flow and a relative humidity meter (Omegaette HH311, Omega Engineering, Stamford, CT, USA). A microscope slide was mounted on the chamber wall in such a way that the cryostream could be blocked without opening the chamber. In this way, the relative humidity of the gas that contacts the crystal during the blocking phase could be controlled to better than 5%.

The principal experimental setups used were (i) a home source (λ = 1.54 Å, Rigaku RuHR generator, Rigaku R-AXIS IV image-plate detector, Rigaku X-stream cryo-cooling system) and (ii) the Stanford Synchrotron Radiation Laboratory (SSRL) beamline 7-1 (λ = 1.08 Å, with MAR Research MAR345 image-plate detector and SSRL cryo-cooling system). Additionally, SSRL beamline 9-2 and Advanced Light Source (ALS) beamlines 5.0.2, 5.0.3 and 8.2.2 (λ = 1.0 Å, with Area Detector Systems Corporation Quantum 4, Quantum 210, Quantum 4 and Quantum 315 CCD detectors and Oxford Cryosystems Cryosystem 600) were used for measuring crystal parameters as a function of cryoprotectant concentration. The detector was typically positioned such that the resolution at the outer edge was 1.8 Å.

For each data point, several images were collected: five for thermolysin and two wedges of four to ten frames, each wedge separated by 90°, for β-galactosidase. The frame width was 1.0° for thermolysin and 0.3–0.5° for β-galactosidase. These images were then processed using *MOSFLM* (Leslie, 1992) in order to extract unit-cell parameters, mosaicity and signal to noise. The crystal space groups are $P2_12_12_1$ for β-galactosidase and $P6_122$ for thermolysin. In neither case was there evidence for a change in symmetry with cryocooling.

2.3. Measurements of cryosolvent density

For bulk-solvent density measurements at room temperature, a 50 ml volumetric flask and a 0.01 mg balance were used. Only one measurement was made at each cryoprotectant concentration, since the uncertainty in the room-temperature density was five to ten times smaller than that at low temperature. Solutions were prepared gravimetrically by first measuring the density of the mother liquor with no cryoprotectant and the density of the pure cryoprotectant. A solution of x% (by volume) cryoprotectant and $(100 - x)$% mother liquor was then prepared by weighing the correct amounts of cryoprotectant, mother liquor and water. For measurements at low temperature, a buoyancy-based procedure using liquid nitrogen as the displaced liquid was developed (Dewar, 1902). A small polyethylene tube (internal diameter $\simeq$ 4.0 mm) was constructed from a transfer pipet (Fisherbrand 13-711-9A; Fisher Scientific, Pittsburgh, PA, USA) by cutting off the bulb and melting the other end closed. Fishing line was then attached to the ends of the tube, allowing it to be suspended beneath a balance (MX5; Mettler-Toledo, Columbus, OH, USA), so that the tube ran horizontally. After zeroing the balance, a known volume (*e.g.* 0.7 ml) of the bulk solvent of interest was transferred to the tube using a syringe. The weight of the tube was then measured both in air and suspended in approximately a litre of liquid nitrogen in a cryogenic Dewar (Hampton Research). These measurements were used to determined the density of the bulk solvent at 77 K according to the relationship

$$\rho = W_{\rm air}^{\rm bs}/v = W_{\rm air}^{\rm bs}\rho_{\rm N_2}/W^{\rm N_2}, \qquad (1)$$

where $W_{\rm air}^{\rm bs}$ is the weight of the bulk solvent, v is the volume of the bulk solvent at low temperature, $\rho_{\rm N_2}$ is the density of liquid nitrogen at 77.5 K (0.806 g ml^{-1}) and $W^{\rm N_2}$ is the weight of liquid nitrogen displaced by the bulk solvent. From Archimedes' principle, $W^{\rm N_2}$ is given by the difference in weight between the empty tube suspended in liquid nitrogen and the cryosolvent-containing tube suspended in the same liquid.

Operationally, two problems were encountered by having the liquid nitrogen at its boiling point. Firstly, bubbles produced perturbations which increased the uncertainty in the weight measurement. Secondly, and more problematically, in some cases bubbles were produced inside the tube, which could introduce large errors in the measured weight. Whether

Table 1
Summary of the X-ray data-sets used to delineate crystal behavior in the presence of different cryosolvents.

Protein	Cryoprotectant	Temperature (K)	No. of cryoprotectant concentrations tested	Mean No. of crystals tested† at each concentration
Thermolysin	Glucose + oil	100	10	4.9
Thermolysin	Glucose only	100	5	3.2
Thermolysin	Glucose only	300	8	2.3
β-Galactosidase	DMSO	100	8	3.3
β-Galactosidase	DMSO	300	6	1.2
β-Galactosidase	PEG 400	100	4	1.0
β-Galactosidase	PEG 400	300	8	2.3

† X-ray data were measured for each crystal as explained in the text.

these bubbles occurred depended both on the cryoprotectant and on its concentration. To address these problems, the nitrogen Dewar was placed in a bell jar attached to a vacuum pump for about 10 min, which cooled the nitrogen to approximately 74 K. The tube was then plunged into this 'supercooled' nitrogen and the weight was monitored as the nitrogen was warmed to boiling. The weight at the boiling point was then determined either by averaging over a few minutes at the final temperature or, in cases where this procedure was prevented by bubbles forming in the tube, by extrapolating to the final temperature (∼77.5 K). The two situations can easily be distinguished by a sudden change in the weight with the formation of bubbles inside the tube. Three to ten measurements were made for each cryoprotectant concentration. The uncertainty in the calculated density at low temperature ranged from ±0.005 to ±0.015 g ml^{-1}, dependent in part on whether the submerged weight needed to be extrapolated. The uncertainty in the room-temperature density was typically about ±0.002 g ml^{-1}. Additionally, the whole process was carried out in a chamber filled with nitrogen gas in order to minimize condensation and ice formation on the thread supporting the tube.

Measurements were carried out on mixtures of the mother liquors for the two crystals and their cryoprotectants over a range of cryoprotectant concentrations. In the case of β-galactosidase, PEG 8000 was omitted from the solutions because this molecule is probably too large to penetrate into the solvent channels of the crystal. Additionally, measurements were carried out on binary mixtures of water and the following cryoprotectants: DMSO, PEG 400, glucose, glycerol, 2-methyl-2,4-pentanediol (MPD, Eastman Kodak) and 2,3-butanediol (Sigma).

3. Results

3.1. Effect of the cryoprotectant on the crystal lattice at room temperature

The effect of the cryoprotectant on lattice parameters and diffraction quality was explored by equilibrating several crystals to different cryoprotectant concentrations and measuring the diffraction as described in §2. The number of crystals tested for each condition varied from one to nine. The tests carried out are summarized in Table 1. Thermolysin has the best coverage, while β-galactosidase with PEG 400 has the worst.

In each of the three cases studied here, namely β-galactosidase with DMSO, β-galactosidase with PEG 400 and thermolysin with glucose, the cryoprotectant has a slightly different effect on the room-temperature lattice parameters and the diffraction quality. For β-galactosidase with DMSO, the unit-cell volume decreases with increasing amounts of DMSO up to 35%(*v*/*v*) (Fig. 1). The mosaicity is not affected very much (increasing less than 50%) and the crystals appear to be more radiation-sensitive (data not shown). At 50%(*v*/*v*) DMSO, the crystals no longer diffract. For β-galactosidase with PEG 400, there is a distinct change of about 2% in the unit-cell volume at approximately 35%(*v*/*v*) PEG 400 (Fig. 1*a*). In contrast to the results with β-galactosidase, the room-

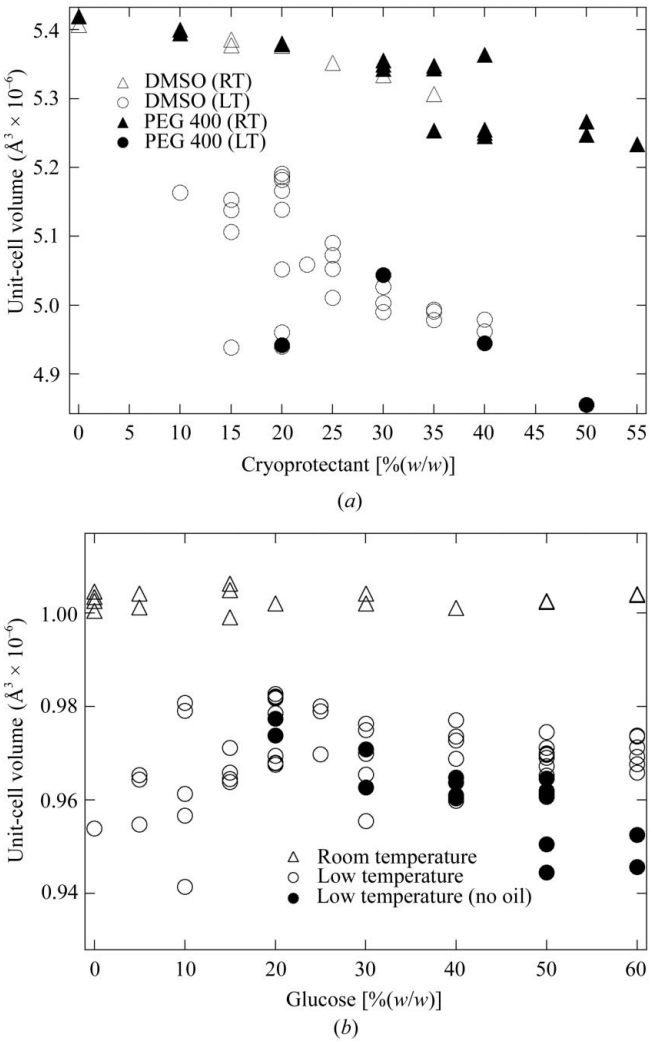

Figure 1
(*a*) Dependence of the unit-cell volume of β-galactosidase crystals on cryoprotectant concentration. The triangles denote crystals at room temperature and the circles denote flash-cooled crystals at low temperature. (*b*) Dependence of the unit-cell volume of thermolysin crystals on cryoprotectant at room temperature (triangles) and at low temperature (circles).

temperature thermolysin lattice parameters appear to be largely unaffected by the cryoprotectant glucose (Fig. 1*b*).

3.2. Effect of cryoprotectant on the lattice at low temperature

In all cases, cooling has a larger effect on the lattice parameters than does the addition of cryoprotectant at room temperature (Figs. 1*a* and 1*b*). The effects are variable, but the trend seems clear. For β-galactosidase, the unit-cell volume decreases by ~4–8% and seems to depend on the amount of cryoprotectant. For thermolysin, the unit-cell volume decrease is typically 2–6% and does not obviously depend on the amount of glucose present.

3.3. Optimal cryoprotectant concentration for flash-cooling

With the β-galactosidase crystals, there is a cryoprotectant concentration that optimizes diffraction quality following flash-cooling. Optimization occurs at roughly 30%(*v*/*v*) DMSO or 40%(*v*/*v*) PEG 400 (data not shown). Below the optimum the diffraction is poor, with diffuse scatter, poorly shaped spots, a lower diffraction limit and some ice rings. Above the optimum, the diffraction is similarly poor, although there are no ice rings. Even at the optimum there is usually some disruption of lattice order, with the mosaicity typically increasing from 0.2° at room temperature to 0.4° at low temperature.

With the thermolysin crystals, the best results were obtained using glucose as cryoprotectant in concert with Fomblin YR-1800 to remove the mother liquor from the outside of the crystals. With this combination, the optimal glucose concentration was ~60%(*w*/*v*), which is the solubility limit of the sugar. At this concentration, the mosaicity of the flash-cooled crystals was occasionally the same as that at room temperature. Below this concentration, the mosaicity was higher and the diffraction limit was lower. Without the Fombin YR-1800, the results were quite different. The diffraction quality was lower at all glucose concentrations and the unit-cell volumes differed from those obtained with Fomblin YR-1800.

In all three cases, the degradation in diffraction quality appears to mainly be a consequence of cryocooling, as the room-temperature diffraction is only marginally affected by the cryoprotectant.

3.4. Annealing and water transport

Fig. 2 shows the results from a typical annealing experiment. A β-galactosidase crystal was equilibrated to 35%(*v*/*v*) DMSO (slightly above the optimal concentration) and flash-cooled in the cryostream. The annealing process described above was then carried out using a blocking time of 2–3 s. Over the first few cycles between low temperature and room temperature (lt–rt cycles), the diffraction quality improved, with the spots becoming less diffuse. The signal to noise increased and the mosaicity fell (Fig. 2*a*). During subsequent cycles, the diffraction quality degraded. The resolution limit decreased, the mosaicity increased and eventually ice rings started to form.

Similar results were observed with PEG 400 as the cryoprotectant, starting above its optimal concentration of 40%(*v*/*v*). Crystals that were equilibrated to slightly below the optimal concentration of either DMSO or PEG 400 could also be improved with the annealing procedure, but the results were less dramatic and generally required longer blocking times (data not shown).

Concomitant with the changes in diffraction quality, the cycling between low and room temperature produced changes in the low-temperature unit-cell volume. For example, in the first experiment described above, the low-temperature unit-cell volume increased on average by 0.2% with each lt–rt–lt cycle. As can be seen in the insets to Fig. 2(*b*), the increase is not uniform for all of the unit-cell parameters. This result will be discussed below.

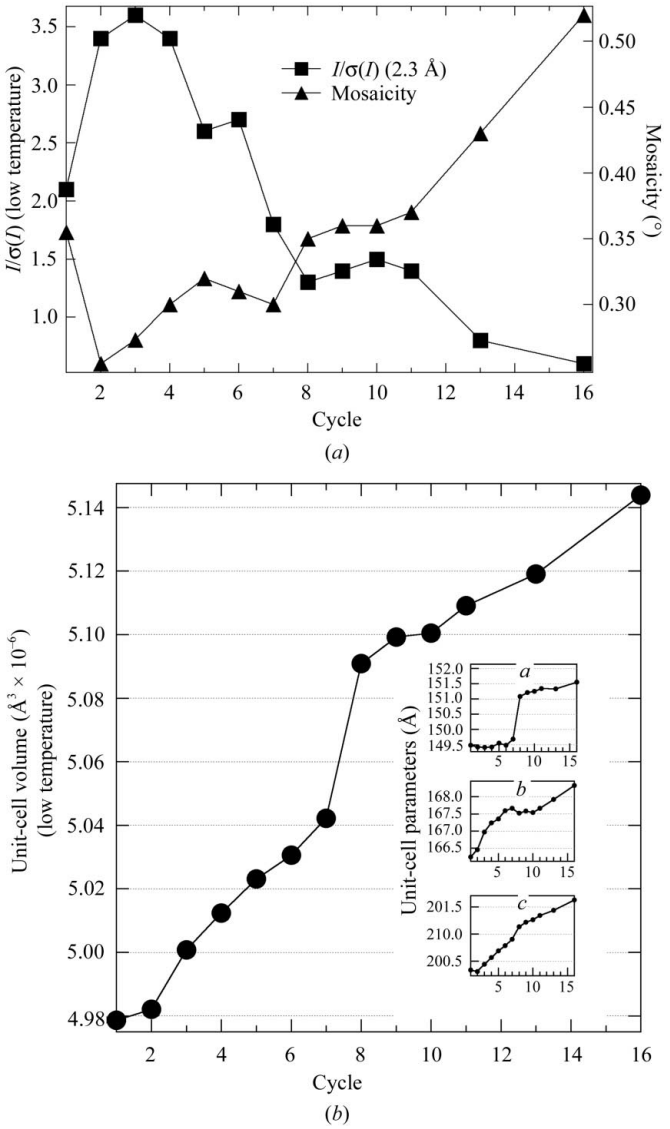

Figure 2
Evolution of crystal parameters over 16 cycles of lt–rt cycling of a crystal of β-galactosidase with DMSO as cryoprotectant, starting at ~35%(*v*/*v*). (*a*) Change in mosaicity (triangles) and $I/\sigma(I)$ (squares) for data to 2.3 Å resolution. (*b*) Changes in unit-cell volume and, in the inset graphs, the individual unit-cell parameters. Experimental setup: SSRL 7-1.

To investigate the unit-cell volume increase further, a similar experiment was performed under different humidity conditions, with a chamber for humidity control. Fig. 3(*a*) shows that 100% relative humidity (RH) produced the largest volume change. Decreasing the RH decreased the volume change until about 25% RH was reached. At this humidity, the volume remained roughly constant (for the blocking time of 4 s used in this experiment). At 4% RH, the volume decreased.

A similar experiment was performed by varying the melt time but keeping the relative humidity essentially constant, using the ambient humidity in the hutch (about 50% RH; Fig. 3*b*). There was an inverse correlation between the melt time and the unit-cell volume.

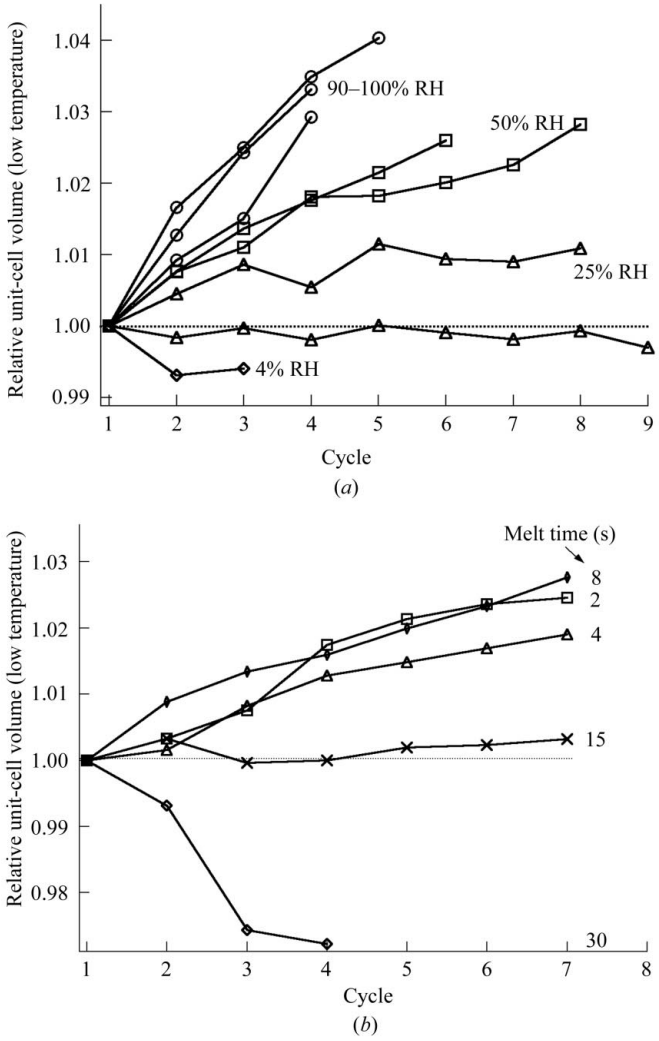

Figure 3
Repeated experiments with different crystals showing the effect of the relative humidity (RH) on the unit-cell volume change during lt–rt cycling. All crystals were initially at 30%(*v*/*v*) DMSO. (*a*) The effect of changing the RH with a constant melt time of 4 s (circles, 90–100% RH; squares, 50% RH; triangles, 25% RH; diamonds, 4% RH). Experimental setup: home source. (*b*) The effect of changing the melt time with constant RH (~50%). For clarity, additional trials at 2, 4 and 8 s have been omitted, but the results were similar; all three have comparable slopes. Experimental setup: SSRL 7-1.

The melt-time experiment was also performed with the β-galactosidase/PEG 400 system, using eight crystals with melt times varying from 1 to 15 s. The humidity-control experiment was performed with the thermolysin/glucose system, using five crystals with relative humidities from 10 to 65%. In both cases, the results (not shown) were qualitatively similar to those described above.

Additionally, melt-time experiments were performed on both β-galactosidase systems with the addition of a layer of Paratone surrounding the crystal (not shown). The presence of the Paratone greatly reduced the unit-cell volume change, suggesting that the Paratone forms a kinetic barrier to water transport during the melting phase.

3.5. Bulk-solvent density

It has been suggested that one reason why cryocooling can be damaging to protein crystals is because of a mismatch in thermal expansion between the protein lattice and the bulk solvent (Juers & Matthews, 2001; Kriminski *et al.*, 2002). Initial measurements of the thermal expansion of the bulk solvent using the method described above near the optimal DMSO concentration for β-galactosidase were consistent with this idea. Since the annealing experiments appear to alter the water content of the crystal and therefore the composition of the bulk solvent, it is important to know how the thermal expansion of the bulk solvent depends on its composition.

Fig. 4(*a*) shows the change on cooling of the specific volume of the three bulk solvents used in these experiments as a function of cryoprotectant concentration. In each case, there is a discontinuity between ~30 and 40% cryoprotectant. At concentrations higher than 40% there is vitrification of the solvent, whereas below the discontinuity ice forms during cooling. Such ice formation could easily be recognized in that the liquid turned opaque during cooling. At the higher concentrations of cryoprotectant, no such opacity was observed. The correlation between opacity and ice formation was verified with control experiments in which mixtures of DMSO and water were flash-cooled in cryoloops. When white opacity was observed, X-ray scattering showed a powder diffraction pattern for hexagonal ice. If there was no opacity, then only diffuse rings were observed.

Fig. 4(*b*) shows the change in specific volume on flash-cooling for some cryoprotectant mixtures not included in Fig. 4(*a*). These also typically show a discontinuity between ~20 and 40% cryoprotectant.

4. Discussion

4.1. Optimal cryoprotectant concentration

In the cases reported here, there is an optimal cryoprotectant concentration for best diffraction at low temperature. This is a common observation, which has been quantified in at least one other case (Mitchell & Garman, 1994). Generally, above and below the optimum, the mosaicity is higher, the diffraction limit lower and the signal to noise poorer.

It has been suggested that optimal cryoprotection is achieved when the contraction of the bulk solvent correctly compensates for the contraction of the lattice and the protein (Juers & Matthews, 2001; Kriminski *et al.*, 2002). This compensation can be quantified with the following expression (Juers & Matthews, 2001):

$$\nu_{\rm exit} = \Delta_{\rm sol} + (\nu_{\rm prot}\Delta_{\rm prot} - \Delta_{\rm cell})\,(1 - \Delta_{\rm sol})/(1 - \nu_{\rm prot}). \quad (2)$$

The quantity $\nu_{\rm exit}$ represents the fraction of the bulk solvent that exits the unit cell of the crystal on cryocooling. $\Delta_{\rm sol}$ is the fractional change in the specific volume of the bulk solvent on cooling, $\Delta_{\rm cell}$ and $\Delta_{\rm protein}$ are the fractional changes in the unit-cell volume and protein volume, and $\nu_{\rm prot}$ is the fraction of the unit-cell volume occupied by the protein at room temperature. If, on cooling, the respective contractions of the bulk solvent, the unit cell and the protein all compensate for each other, $\nu_{\rm exit}$ should be zero. In contrast, a non-zero value of $\nu_{\rm exit}$ suggests that bulk solvent is expelled from or imported into the unit cell during cooling, damaging the lattice in the process.

Using the known crystal structures of β-galactosidase and thermolysin, the unit-cell parameters from Fig. 1 and the bulk-solvent thermal expansions shown in Fig. 4(*a*), the calculated values of $\nu_{\rm exit}$ were determined (Fig. 5). The figure shows not only the calculated amount of solvent exiting the crystal but also the changes in unit-cell volume and specific volume of bulk solvent as a function of cryoprotectant concentration. Whether the bulk solvent can accommodate the unit-cell contraction depends on the value of $\nu_{\rm exit}$. Although $\nu_{\rm exit}$ never reaches zero, the smallest values occur near the optimal cryoprotectant concentration. This fact suggests that at the optimal cryoprotectant concentration the bulk-solvent contraction best compensates for the lattice and protein contractions. The slightly positive values of $\nu_{\rm exit}$ seen in Fig. 5 suggest that either a small amount of bulk solvent is extruded out of the unit cells during cooling or perhaps the model being used does not completely characterize the process.

One consideration is that the liquid in the solvent channels in the crystal may not behave in the same way as bulk solvent. This outcome is especially likely at lower cryoprotectant concentrations, where ice may form in the bulk sample but vitrification may occur in the solvent channels of the crystal. It may be that contraction by the protein lattice during cooling might increase the density of the solvent relative to its behavior in bulk. The cooling rate in the crystal is likely to be greater than that during the density measurements, possibly enhancing solvent contraction in the crystal. These possibilities notwithstanding, the measurements reported here are consistent with the idea that the optimal cryoprotectant concentration matches the contraction of the bulk solvent to the contraction of the protein and the lattice.

Kriminski *et al.* (2002) have suggested that flash-cooling may occur too rapidly for the bulk solvent to exit the crystal completely. Instead, they suggest that the bulk solvent is expelled into small regions scattered throughout the crystal. The distance that the solvent can be transported through the crystal during cooling depends on several factors, including the sequence in which lattice repacking and solvent vitrification occur. The degree to which the solvent completely exits the crystal or is localized to small pools depends on the particulars of each system. In agreement with Kriminski *et al.* (2002), however, it would seem that the solvent may not be free to exit the crystal completely during cooling. Similarly, in the case that the solvent contracts too much, there may not be sufficient time to import solvent throughout the crystal. Here the crystal probably collapses onto itself, degrading lattice order.

4.2. Effectiveness of cryoprotectants

Fig. 4(*b*) shows the thermal contraction of various cryoprotectants on flash-cooling. That DMSO undergoes greater

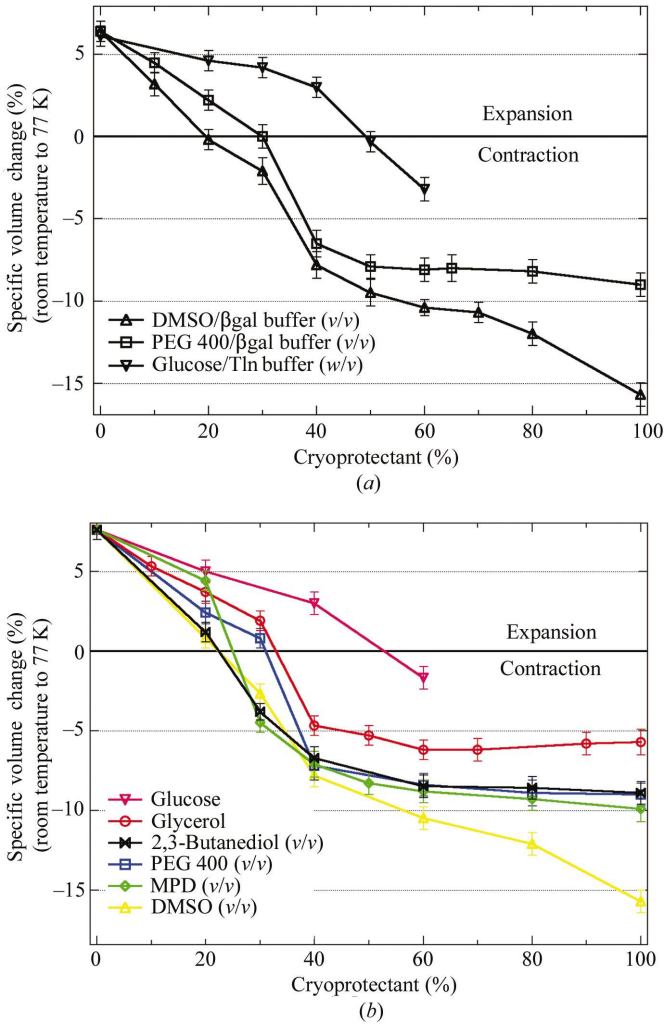

Figure 4
The change in specific volume of various cryosolvent solutions between room temperature and 77 K as a function of cryoprotectant concentration. (*a*) Specific-volume changes for the bulk solvents in the three crystal systems studied in this report. βgal, β-galactoside; Tln, thermolysin. (*b*) Specific volume changes for binary mixtures between water and six different cryoprotectants. Each plotted point is based on the room-temperature value and an average of three to ten low-temperature measurements. The error bars represent average measurement uncertainties and are somewhat larger than either the average deviation or the standard error of the mean.

contraction than PEG 400 at the same concentration is consistent with the observation that lower concentrations of DMSO are required to successfully flash-cool β-galactosidase crystals. Similarly, as can be seen from the figure, the maximum possible concentration of glucose is still not sufficient to give the 7–8% contraction apparently required to successfully cryocool β-galactosidase crystals.

4.3. Water transport and annealing

Typically, when the cold stream is blocked, the crystal first becomes cloudy and then clarifies. The time for this transition is ~1–2 s, depending on the size of the crystal and the volume of the surrounding liquid. If the crystal is recooled before clearing, ice rings appear in the diffraction pattern and the unit-cell parameters are unchanged. Longer thawing and recooling subsequently eliminates these ice rings and produces a unit-cell increase. This result suggests that the clouding is a surface phenomenon and arises from either (i) condensation and freezing of water vapor from the air onto the surface of the cold crystal or (ii) the formation of ice while thawing the surface mother liquor. The clearing results from the melting of this layer of ice crystals on the surface, which in turn suggests that once the crystal has cleared, its surface, at least, is close to room temperature.

In either case, water will condense from the atmosphere onto the crystal surface and then both diffuse into the crystal and evaporate. These two processes compete to determine whether there is a net flow of water into or out of the crystal by the time it is recooled. Which process dominates depends on several factors, including the relative humidity, the melting time and the hygroscopy of the crystal and the bulk solvent.

If there is a net flow of water into the crystal, the bulk solvent in the solvent channels tends to contract less with cooling, in part because the cryoprotectant concentration is lower (Figs. 4*a* and 4*b*) and also because there is more liquid in the solvent channels. This process favors a relative increase (or a reduced decrease) in the unit-cell volume on cooling. If there is a net flow of water out of the crystal, the opposite situation results, with an increase in the cryoprotectant concentration, greater bulk-solvent contraction and an enhanced decrease in the unit-cell volume.

Whether the diffraction improves or degrades with annealing depends on the cryoprotectant concentration. If it is initially too high, then the bulk solvent contracts too much. A flow of water into the crystal during annealing will favor reduced solvent contraction and is likely to improve lattice

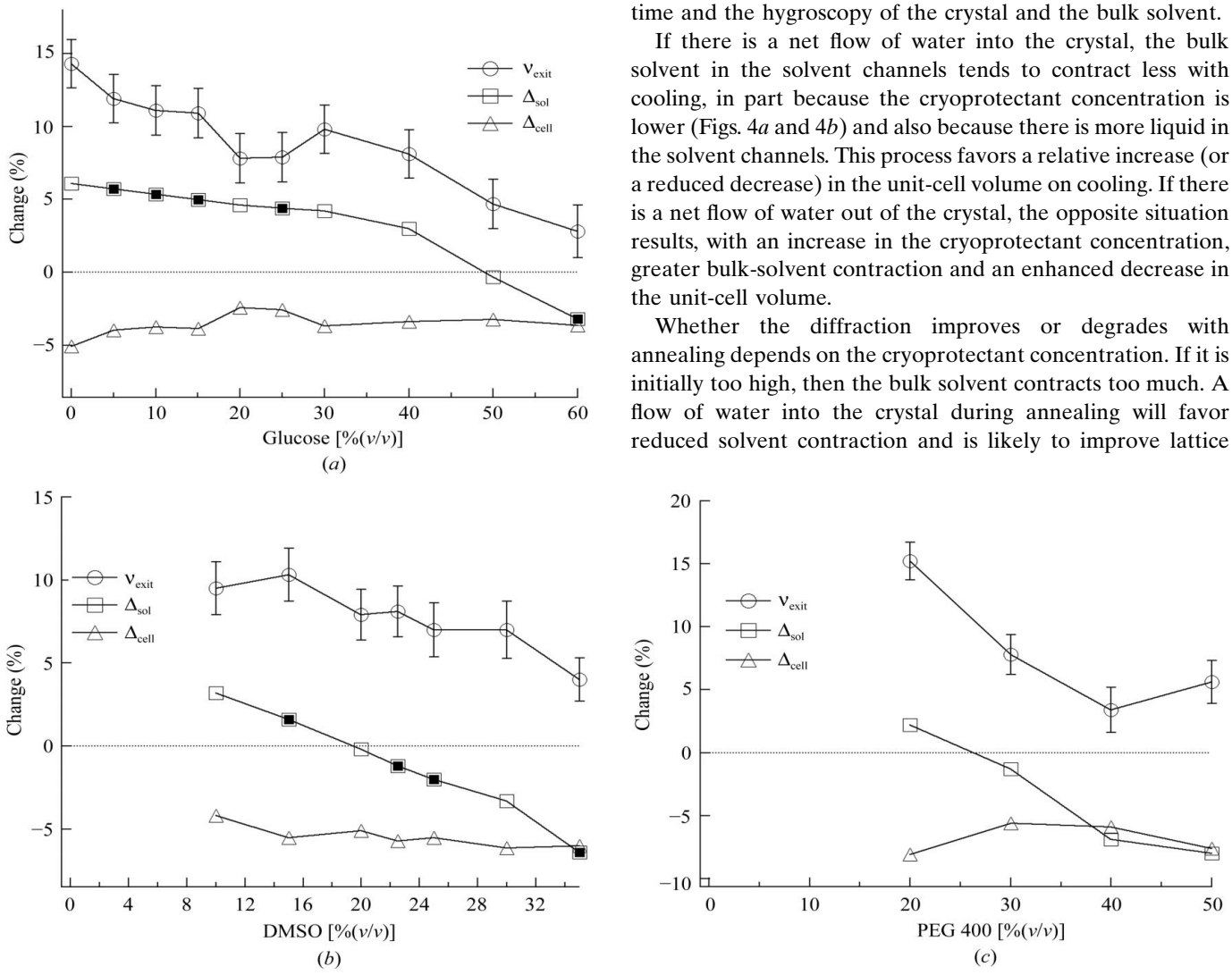

Figure 5
Changes on cooling of the unit-cell volume (Δ_{cell}), change in the specific volume of the bulk solvent (Δ_{sol}) and the calculated solvent expelled from the crystal (ν_{exit}) as a function of cryoprotectant concentration. At concentrations for which Δ_{sol} was not measured, it was interpolated (filled symbols) and these values were then used to calculate ν_{exit}. In the case of β-galactosidase, the effect of excluding PEG 8000 from the solvent channels was corrected for, which slightly increases the value of Δ_{sol} used in (2). Uncertainties in Δ_{sol} and Δ_{cell} are of the order of the symbol size. Error bars in ν_{exit} reflect the uncertainties in the measurement of the quantities given in (2). A potentially greater error comes from the likelihood that the thermal behavior of the solvent in bulk may differ from its behavior in the crystal. (*a*) Thermolysin with glucose. (*b*) β-galactosidase with DMSO. (*c*) β-Galactosidase with PEG 400.

order during the next cooling cycle. Similarly, we might expect that if the cryoprotectant concentration was initially too low, then flow of water out of the crystal during the melt cycle should improve the lattice order during the next cooling cycle.

In practice, we have had much more success with improving the diffraction when the cryoprotectant concentration is initially too high (rather than too low). This result suggests that the lattice damage created when the cryoprotectant concentration is too low is different from the damage created when the concentration is too high. In the latter case, the disorder presumably comes from the molecules collapsing on themselves, which is apparently more reversible than the damage from the expulsion of bulk solvent from the unit cell (or from the crystal as a whole).

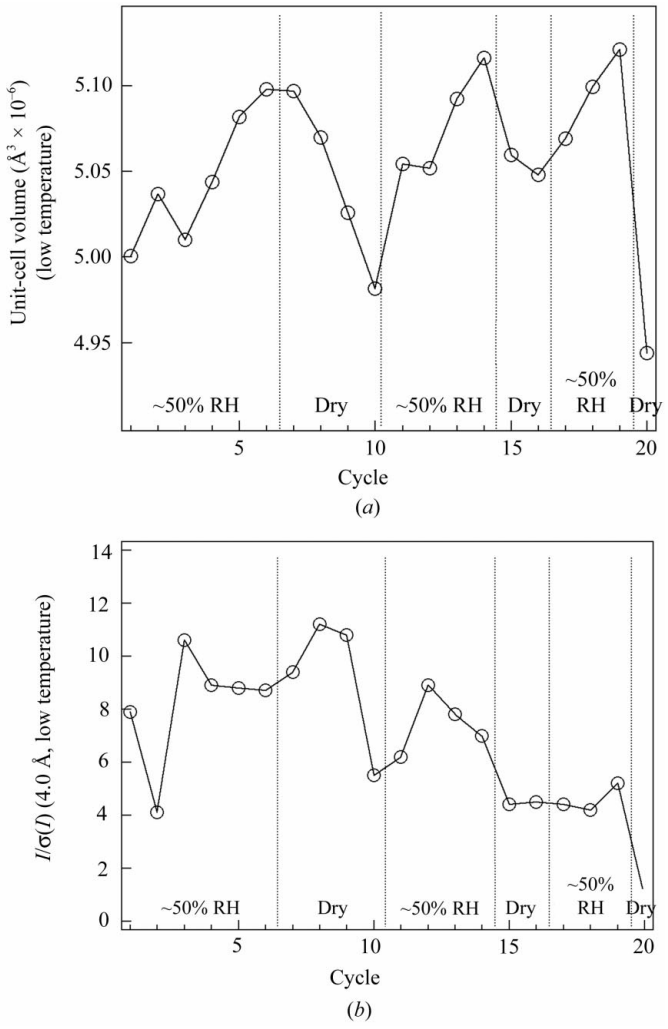

Figure 6
Evolution of crystal parameters for a crystal of β-galactosidase subjected to lt–rt cycling with different humidity conditions (see text for additional details). The crystal was equilibrated to 35%(*v*/*v*) DMSO (slightly above the optimal of 30%) prior to the experiment. (*a*) Changes in unit-cell volume for a crystal subject to cooling and thawing in an 'ambient' atmosphere (~50% RH) and then in a dry atmosphere. (*b*) Plot showing that data quality, as measured by $I/\sigma(I)$, can initially improve and then deteriorate when the crystal is subject to cooling and thawing in an ambient (~50% RH) atmosphere but also when subject to cooling and thawing in a dry atmosphere. $I/\sigma(I)$ for the highest-resolution shell (4.28–4.00 Å), averaged over eight images, is shown. Experimental setup: SSRL 7-1.

Fig. 6 shows the results of an experiment that demonstrates most of these concepts. A β-galactosidase crystal initially at 35%(*v*/*v*) DMSO was flash-cooled. Subsequently, it was melted and recooled using 3–5 s melt times. In the regions labeled '~50% RH', the crystal was exposed to the ambient atmosphere (~50% relative humidity) during the melt cycle. In the regions labeled 'dry', the crystal was exposed to a dry nitrogen flow during the melt cycle. Fig. 6(*a*) shows that in the more humid regime the unit-cell volume increases, while it decreases in the dry regime, consistent with the model of water transport described above. Fig. 6(*b*) shows that overall data quality, measured by $I/\sigma(I)$, can initially improve in either the ambient region or the dry region, suggesting that the crystal is being moved above and below its ideal cryosolvent concentration. However, there is an overall decrease in data quality throughout the process, suggesting that there is some hysteresis, which leads to lattice degradation that is not reversible, at least with this technique.

This observation raises the question of whether lt–rt cycling is required to reach the best diffraction. It seems possible that if the optimal cryoprotectant concentration is used, the best diffraction may be reached with the first cooling, before lattice degradation has a chance to accumulate. However, the optimal cryoprotectant concentration for any given crystal may depend on factors such as the cooling rate, the crystal size and the cooling regime provided by the particulars of the cryostream and crystal handling/soaking protocol used and thus may be very difficult to predict. It therefore seems likely that a typical crystal may have sub-optimal initial cooling and be subject to improvement with lt–rt cycling, especially if the cryoprotectant concentration is initially too high. In this context, there are at least two questions that remain unanswered. Firstly, it is unclear whether there are cases in which multiple lt–rt cycles are required to achieve the best diffraction, even with the most judiciously chosen cryoprotectant concentration. A related question is whether lt–rt cycling can be used to increase lattice order at low temperature relative to that at room temperature.

4.4. Interplay between the bulk-solvent contraction and lattice contraction

An interesting question is to what extent the low-temperature unit-cell volume is determined by the thermal contraction of the bulk solvent or the particulars of the lattice packing. Fig. 2(*b*) sheds some light on this question. The figure can be split into two regions: cycles 1–7 and cycles 8–16, separated by a discontinuity. Within each region the increase in unit-cell volume is relatively uniform, but the individual unit-cell parameters change in different ways. In both regions the volume increase is mostly a result of changes in the *b* and *c* cell parameters, while *a* remains relatively constant. The jump in the unit-cell volume at cycle 8 mostly arises from change in *a*, suggesting that there are at least two alternative packing arrangements. As water is imported into the solvent channels,

the bulk solvent contracts less and the unit-cell volume increases from cycle to cycle. These changes are accommodated either in the lattice contacts (intermolecular) or perhaps in the contacts within the β-galactosidase tetramer (intramolecular). These contacts can apparently be modulated in such a way as to result in small changes in b and c while maintaining a close to 149.5 Å. At some point (*i.e.* at cycle 8), the solvent does not contract sufficiently to maintain this packing and an alternative arrangement is adopted, which has $a \simeq 151$ Å. At this transition, the change in unit-cell volume is dominated by the lattice packing. Within cycles 1–7 and 8–16, however, it appears that the changes in the unit-cell volume are dominated by the solvent contraction within the constraints of the lattice.

While the packing arrangements discussed above are for low temperature, it may be noted that changing the water content of crystals can also cause dramatic effects on room-temperature packing (Boyes-Watson *et al.*, 1947; Esnouf *et al.*, 1998; Kiefersauer *et al.*, 2000). In our experiments, we obtain no information about the lattice at room temperature during the annealing process, but the results of Esnouf *et al.* (1998) and Kiefersauer *et al.* (2000) underscore the need to consider the possibility that changes may be occurring at room temperature as well as at low temperature.

4.5. The use of cryoprotectants in concert with oils

Generally, flash-cooling is carried out either using an oil such as Paratone to eliminate ice formation in the bulk solvent external to the crystal or with a penetrating cryoprotectant to eliminate ice formation within the crystal. The use of oils in concert with penetrating cryoprotectants has been suggested previously but is less commonly used (Kwong & Liu, 1999). The results here further support the combination of these strategies.

Generally, when a cryoprotectant is used, the amount deemed necessary is that which prevents ice formation in the naked mother liquor (Garman & Mitchell, 1996; McFerrin & Snell, 2002). However, it is possible in some cases that this amount of cryoprotectant causes too much contraction of the bulk solvent. The amount of cryoprotectant for expansion matching may cause ice crystals to form in the bulk solvent surrounding the crystal. In such cases, the use of an oil to eliminate the surface solvent would be useful.

The requirement of high concentrations of glucose in concert with an external oil for cryocooling of thermolysin crystals suggests that the use of oils may be helpful even when there is sufficient cryoprotectant to prevent ice formation. An initial test with the β-galactosidase crystals using PEG 400 in concert with Fomblin YR-1800 also gave positive results. The reason for this result is unclear. Potential explanations include an altered cooling rate, the propagation of 'bulk behavior' into the solvent channels within the crystal and the possibility that the temperature response of the external fluid impacts the lattice and the internal fluid differently.

5. Summary

The results presented here suggest that the benefit from '*in situ*' cryo-annealing occurs at least in part as a result of the modulation of the thermal expansion of the bulk solvent by altering its water content. Furthermore, the results suggest that this method of annealing is more likely to be successful if the cryoprotectant concentration is initially too high, rather than too low. In some cases, the failure of '*in situ*' cryo-annealing may be an indication that the cryoprotectant concentration is too low.

Density measurements of bulk cryosolvents at liquid-nitrogen temperatures support the idea that the optimal cryoprotectant concentration is that which matches the thermal contraction of the mother liquor to that of the protein and the lattice. Finally, the possible use of oils in concert with cryoprotectants as a way of improving diffraction quality is noted.

The authors would like to thank Dr Walt Baase for expert technical assistance and, together with Drs Mike Quillin and Richard Kingston, for helpful discussions. Jim Pflugrath brought Fomblin YR-1800 to our attention. Additionally, we are grateful for the thoughtful comments of the reviewers. This work was supported in part by NIH grant GM20066 to BWM.

References

Boyes-Watson, J., Davidson, E. & Perutz, M. F. (1947). *Proc. R. Soc. London Ser. A*, **191**, 83–132.
Dewar, J. (1902). *Proc. R. Soc. London*, **70**, 237–247.
Esnouf, R. M., Ren, J., Garman, E. F., Somers, D. O'N., Ross, C. K., Jones, E. Y., Stammers, D. K. & Stuart, D. I. (1998). *Acta Cryst.* D**54**, 938–953.
Garman, E. (1999). *Acta Cryst.* D**55**, 1641–1653.
Garman, E. F. & Mitchell, E. P. (1996). *J. Appl. Cryst.* **29**, 584–587.
Garman, E. F. & Schneider, T. R. (1997). *J. Appl. Cryst.* **30**, 211–237.
Haas, D. J. & Rossmann, M. G. (1970). *Acta Cryst.* B**26**, 998–1004.
Harp, J. M., Hanson, B. L., Timm, D. E. & Bunick, G. J. (1999). *Acta Cryst.* D**55**, 1329–1334.
Harp, J. M., Timm, D. E. & Bunick, G. J. (1998). *Acta Cryst.* D**54**, 622–628.
Hausrath, A. C. & Matthews, B. W. (2002). *Acta Cryst.* D**58**, 1002–1007.
Hope, H. (1988). *Acta Cryst.* B**44**, 22–26.
Juers, D. H., Jacobson, R. H., Wigley, D., Zhang, X.-J., Huber, R. E., Tronrud, D. E. & Matthews, B. W. (2000). *Protein Sci.* **9**, 1685–1699.
Juers, D. H. & Matthews, B. W. (2001) *J. Mol. Biol.* **311**, 851–862.
Kiefersauer, R., Than, M. E., Dobbek, H., Gremer, L., Melero, M., Strobl, S., Dias, J. M., Soulimane, T. & Huber, R. (2000). *J. Appl. Cryst.* **33**, 1223–1230.
Kriminski, S., Caylor, C. L., Nonato, M. C., Finkelstein, K. D. & Thorne, R. E. (2002). *Acta Cryst.* D**58**, 459–471.
Kwong, P. D. & Liu, Y. (1999). *J. Appl. Cryst.* **32**, 102–105.
Leslie, A. G. W. (1992). *Jnt CCP4/ESF–EAMCB Newsl. Protein Crystallogr.* **26**.
McFerrin, M. B. & Snell, E. H. (2002). *J. Appl. Cryst.* **35**, 538–545.
Mitchell, E. P. & Garman, E. F. (1994). *J. Appl. Cryst.* **27**, 1070–1074.
Rodgers, D. W. (1994). *Structure*, **2**, 1135–1140.
Sjögren, T., Carlsson, G., Larsson, G., Hajdu, A., Andersson, C., Pettersson, H. & Hajdu, J. (2002). *J. Appl. Cryst.* **35**, 113–116.
Teng, T.-Y. (1990). *J. Appl. Cryst.* **23**, 387–391.
Yeh, J. I. & Hol, W. G. J. (1998). *Acta Cryst.* D**54**, 479–480.